OVERVIEW OF OCEAN BACKGROUND CONDITIONS AND MODELING OF INTERNAL WAVES

Alex Warn-Varnas
SACLANT Research Center, Via S. Bartolomeo 400
19026 La Spezia, Italy

Steve Piacsek
Code 322, Naval Oceanographic and Atmospheric Research Laboratory, Stennis Space Center, MS 39529

INTRODUCTION

In this paper we would like to consider some aspects of the oceanic background and the results of some modeling studies that pertain to the generation and propagation of internal waves in the ocean. We will look at this background state as determined from the various field surveys and will consider the feasibility of modeling these background conditions and phenomena. One of the motivations for the current studies is that the propagation of internal waves is strongly affected by velocity and density gradients and that the ocean exhibits a high spatial and temporal variability of these gradients. This background description encompasses various elements, of which we consider the mixed layer region, the mesoscale variability and associated eddies, fronts, fine structure, and their interaction with internal waves.

EXAMPLES OF INTERNAL WAVE PROPAGATION AND SHEAR

Figure 1 shows the results of the simulation of a collapsing turbulent patch in a large scale oceanic shear field (Piacsek and Roberts, 1975). Note the generation of internal waves indicated by the streamfunction patterns in the form of rays. There is a prescribed mean vertically sheared flow present that moves from left to right. As the collapse progresses, more rays come out and are bent to the right. In the upper right hand side the presence of a critical layer sets up a region into which the waves cannot propagate. On the left side the rays are refracted toward the vertical and undergo reflection at the surface, setting up standing wave-like patterns.

Propagating internal waves have often been observed at the bottom of the mixed layer and in the seasonal thermocline. The results depicted in Figure 2 were obtained with a 200-meter thermistor chain during a 1987 Planet cruise in the Norwegian Sea (Sellschopp, 1987). The top portion of the figure shows the time series of the temperature profile versus depth. The corresponding isotherms are shown in the bottom portion. Note the presence of internal waves at the base of the mixed layer and in the thermocline.

It has been established that shear and internal wave activity depend on certain environmental parameters. These are the Brunt-Vaisala frequency, atmospheric forcing, geostrophic currents, and topography. The conclusions were reached on the basis of field surveys and theoretical considerations (Garrett and Munk, 1979; Ruddick and Joyce, 1979; Brown and Owens, 1981; Briscoe and Weller, 1984).

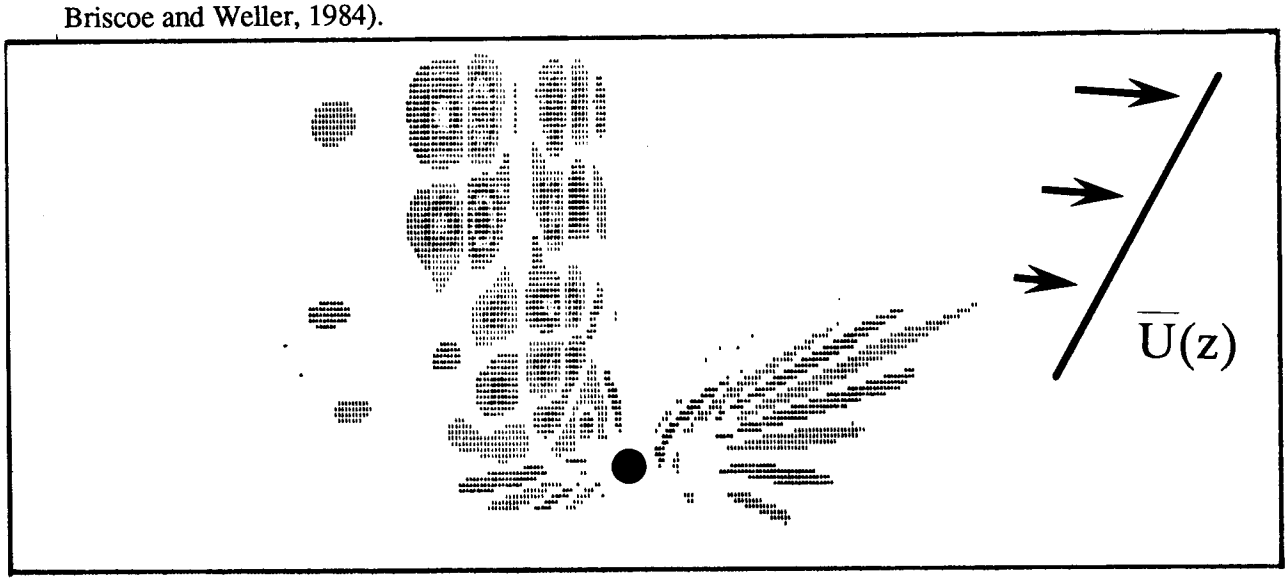

Figure 1. Internal wave generation by a collapsing turbulent patch in a stratified fluid, in the presence of a mean shear (flow from left to right) (Piacsek and Roberts, 1975).

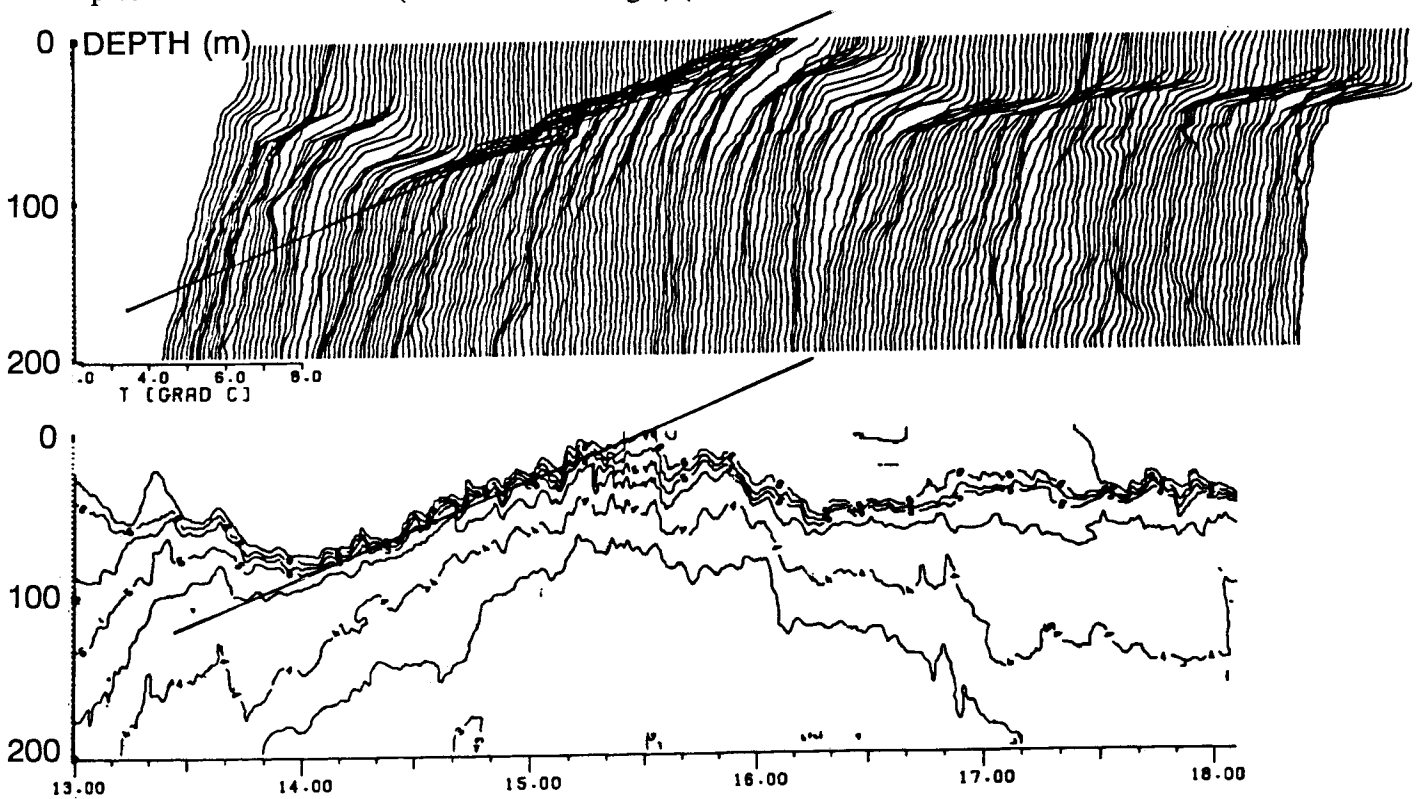

Figure 2. Internal wave propagation at the bottom of the mixed layer and in the seasonal thermocline (Sellschopp, 1987).

Strong vertical geostrophic shears have been measured near fronts using an ADP (acoustic doppler profiler), during the previously mentioned cruise in the Norwegian Sea along a different track. Figure 3 shows the measured shear at the edges and middle of a warm feature. Strong positive shear occurs when passing from cold to warm water (cut a). There is a lack of shear in the middle of the eddy (cut b) and the presence of a negative shear when passing from warm to cold water (cut c). The average vertical shears are about 10^{-3} sec^{-1} in the frontal region, which is about five times smaller than the magnitude found near the base of mixed layers.

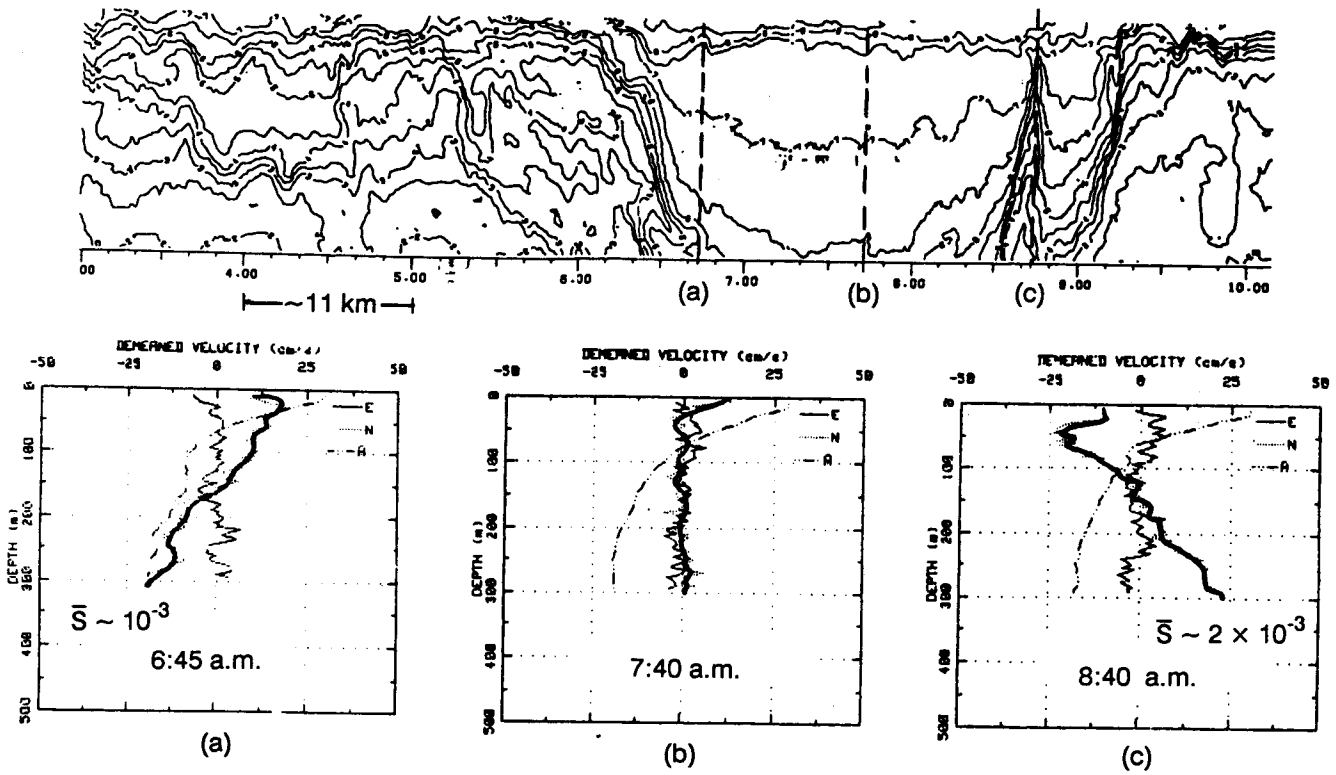

Figure 3. Examples of geostrophic shear, as observed by an acoustic Doppler profiler, in passing into and out of a warm eddy in the Faroe area (Sellschopp, 1987).

An example of strong horizontal geostrophic shear in the confluence region of the Icelandic current and the North Atlantic inflow is shown in Figure 4. Horizontal shears are about 10 cm/sec/10 km, and in some sections can be larger. The results are based on the analysis of the Icelandic Current and the Atlantic Inflow Experiment surveys, carried out by the SACLANT Research Center in 1987 (Hopkins et al. ,1989).

An analysis of the internal wave energy budget has been performed for the JASIN survey data by Briscoe (1983). The results show that sometimes the rate of change of internal wave energy correlates with the mesoscale horizontal shear, the wind, and inertial wave activity (Figure 5). The correlation is not present all the time, however. Part (b) of the figure shows the dependence of

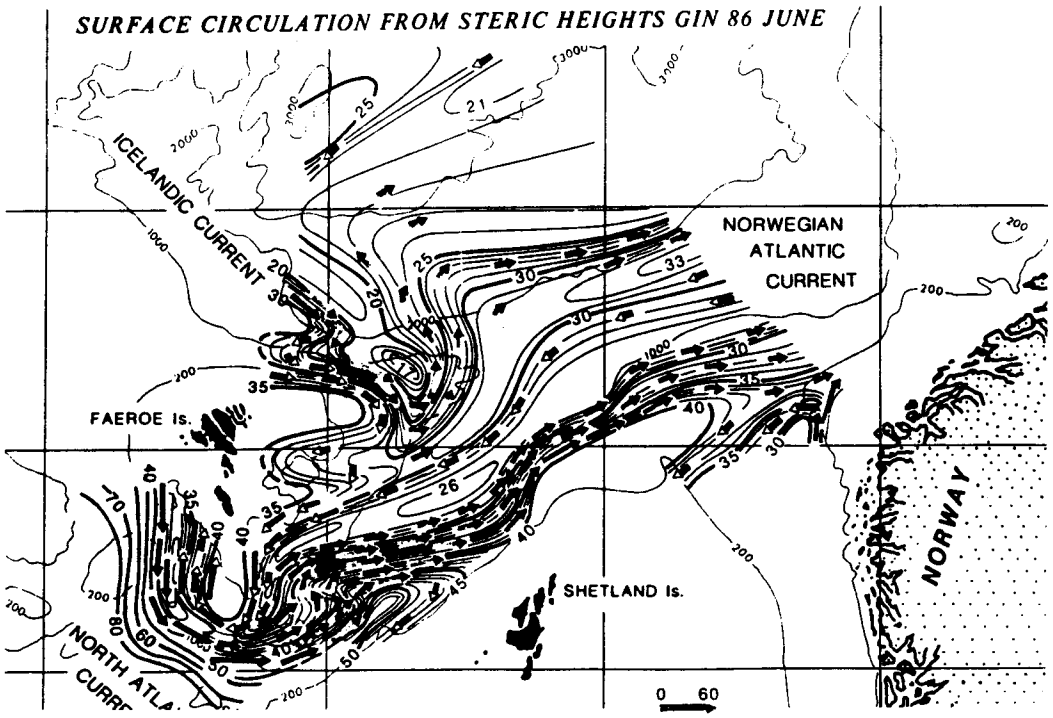

Figure 4. Example of strong horizontal geostrophic surface shears in the North Atlantic Inflow between Faroes and Shetland Islands (Hopkins et al., 1989).

internal wave energy on surface wave amplitude delayed by 11 days. The correlation is very high throughout the measurement period. Internal wave activity exhibits a seasonal variation: the analysis and interpretation of the LOTUS data demonstrate this (Figure 6) (Briscoe and Weller, 1984). Note the marked decrease in internal wave activity during the summer at the 100-500 meter depth levels. Near the surface the decrease occurs in the fall.

Figure 7 shows an example of stepped T,S structures in the Eastern Caribbean region southeast of Barbados observed during the C-SALT experiment (Boyd and Perkins, 1987). The steps gradually increase with depth from about 5 to 30 meters at the 200 to 350-meter depth levels, respectively. The temperature and salinity jumps at the profile 'steps' are thought likely to be set up by strong salt fingering processes; such fingers have actually been observed in the ocean by optical means.

FOCUS OF CURRENT STUDIES

Our current objectives are concerned with the provision of a deterministic forecast (or calculation from forecasted variables) for environmental parameters of interest at resolvable computational scales. For the unresolvable scales statistical predictions of various kinds would be used, adapted, and developed. In such fashion a combined deterministic and statistical information on environmental parameters of interest would be provided.

In the upper ocean successful prediction of the mixed layer behavior has been achieved in situations where the atmospheric forcing activity is dominant vis a vis mesoscale advection. Figure 8 displays

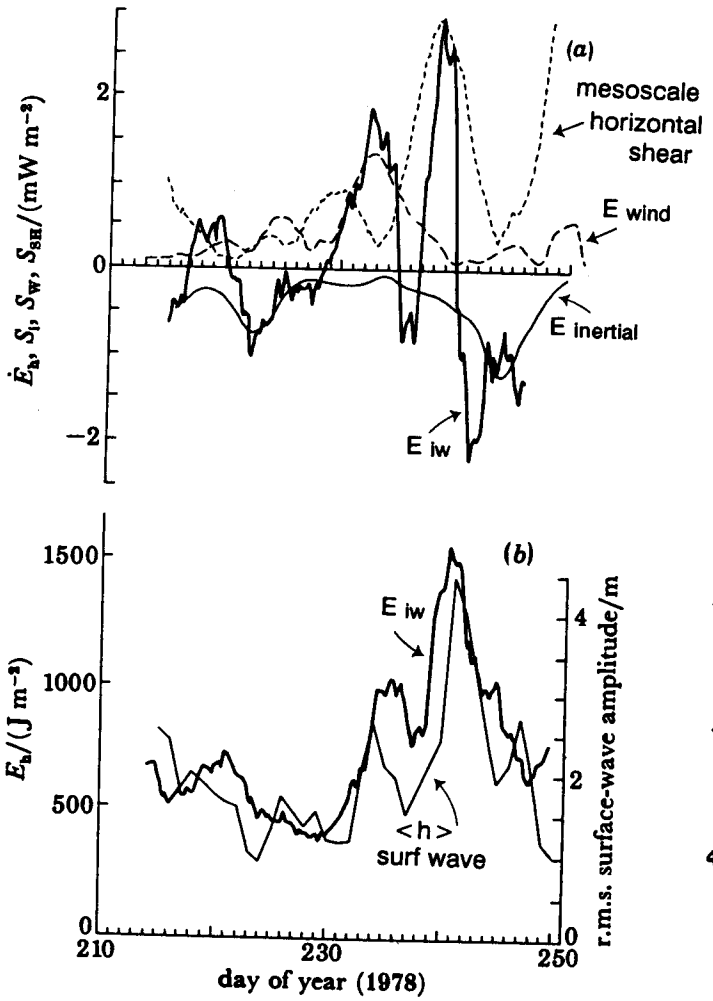

Figure 5. Dependence of internal wave energy on surface forcing during the JASIN experiment in the Northeast Atlantic (Briscoe, 1983).

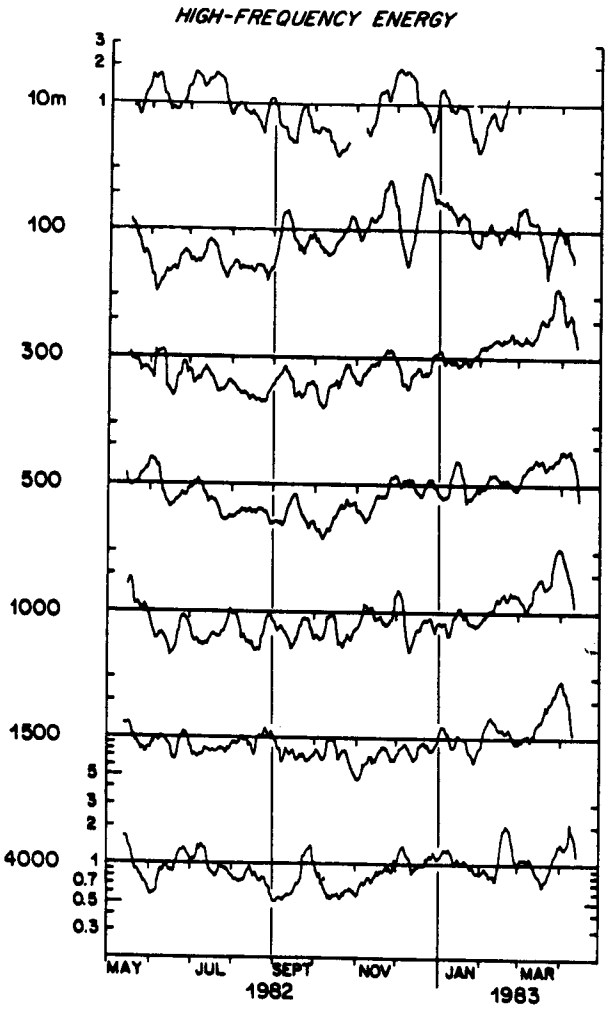

Figure 6. The depth dependence of the seasonal variation of internal wave energy during the LOTUS experiment in the Sargasso Sea (Briscoe and Weller, 1984).

mixed layer simulations with three different models at a former ocean station November (30N, 140W in the Pacific) (Martin, 1985). The Niiler (1975) and Garwood (1977) models are of the 'bulk' type (they assume the existence of a mixed layer and work with the vertically integrated or 'bulk' equations), whereas the Mellor-Yamada model is of a differential type (i.e., set up by differencing on a vertical grid). Initial conditions were set to the temperature profile obtained with an XBT and the atmospheric forcing was derived from meteorological measurements. All the simulations show the seasonal trends in sea surface temperature and mixed layer depth that are observed in the data. However, detailed differences do exist in relation to the data. The models show a quicker spring transition. The ML2 model mixes down less deep in the winter than the other two and is more at variance with the data.

Simulations of mixed layer behavior that resolved the diurnal (Price et al., 1986) and synoptic time scale (Warn-Varnas et al., 1981)]were also performed. Some investigators studied the mixed layer

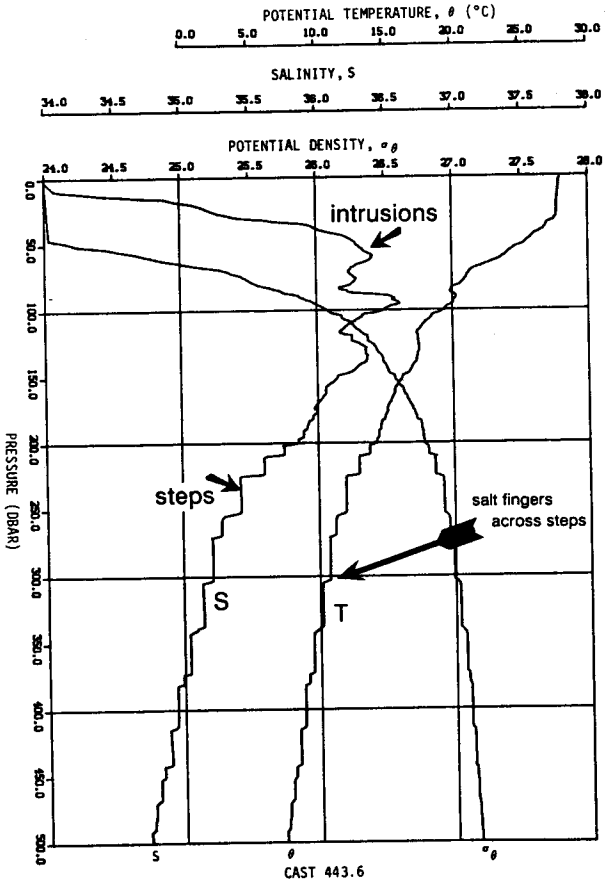

Figure 7. Step structures in temperature and salinity profiles as observed in the C-SALT experiment off Barbados Boyd and Perkins, 1987).

response to hurricanes (Martin, 1982; Price, 1981). Figure 9 shows one such study for hurricane Eloise that occurred in the Gulf of Mexico. A comparison is shown between the predicted and measured u and v velocity components. The measurements were made by the NDBO buoy EB-10. Both phase and amplitude show agreement with data with some slight differences.

A system to predict regional mesoscale behavior has been developed by the Harvard University group (Robinson et al., 1986). The dynamical model is initialized from field survey data and is forced by observed boundary conditions. Data can be assimilated into the model. The boundary conditions play a crucial role in the forecast. Figure 10 displays dynamical simulations of the California Current with such a system. Note that on day 14, the simulation with the boundary condition obtained by linear interpolation of the measurements gives agreement with the data. The persistence boundary conditions leads to substantial deviations from the actual observed state.

At present a capability has been developed to predict various environmental parameters in conjunction with a real-time upper ocean nowcasting system that is operational at FNOC (Fleet Numerical Oceanographic Center) (Clancy and Pollak, 1983). Other prediction systems and approaches for describing environmental parameters of interest exist in research environments.

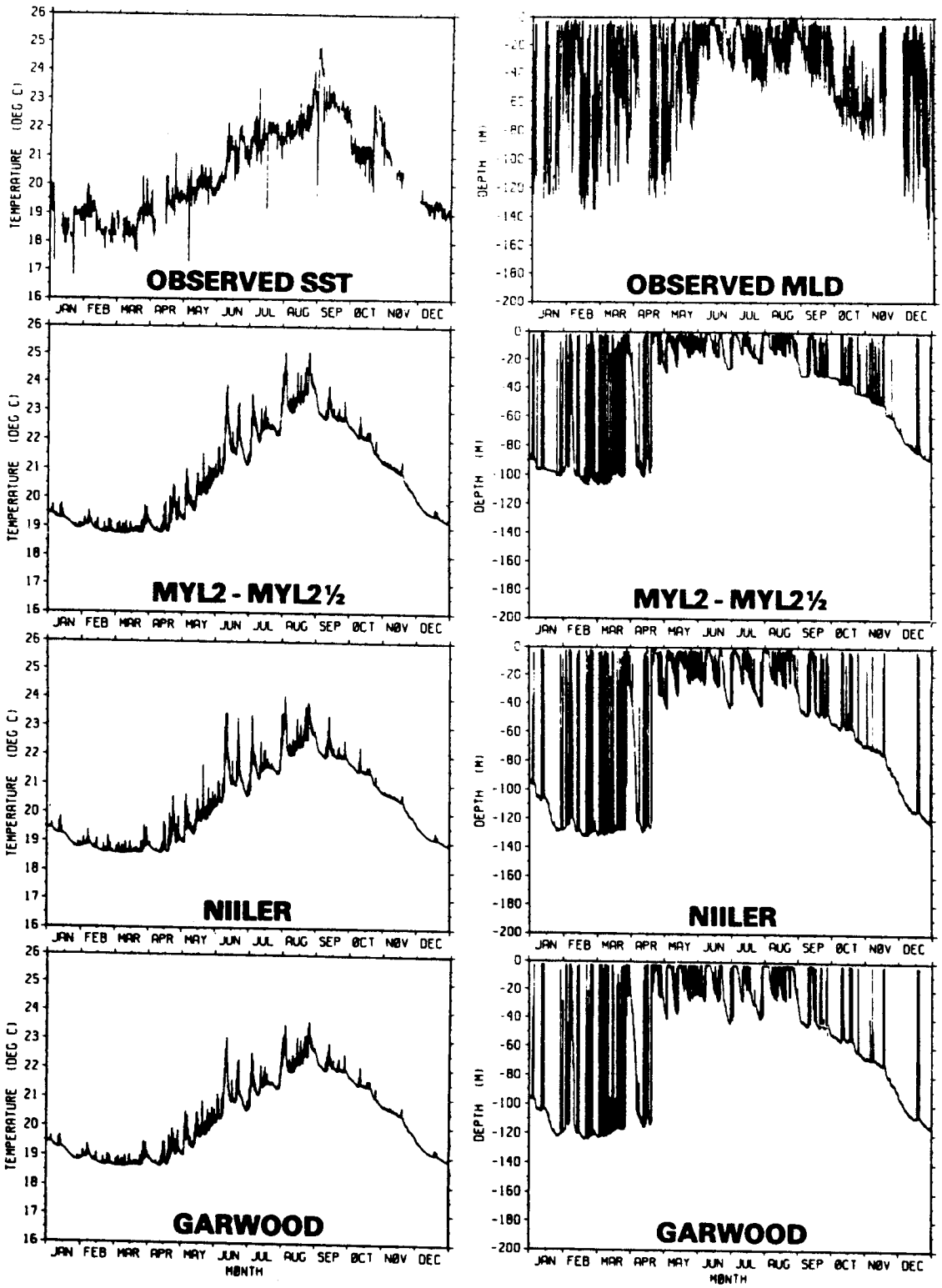

Figure 8. Mixed layer simulation with different models at weather ship November in the Pacific (Martin, 1985).

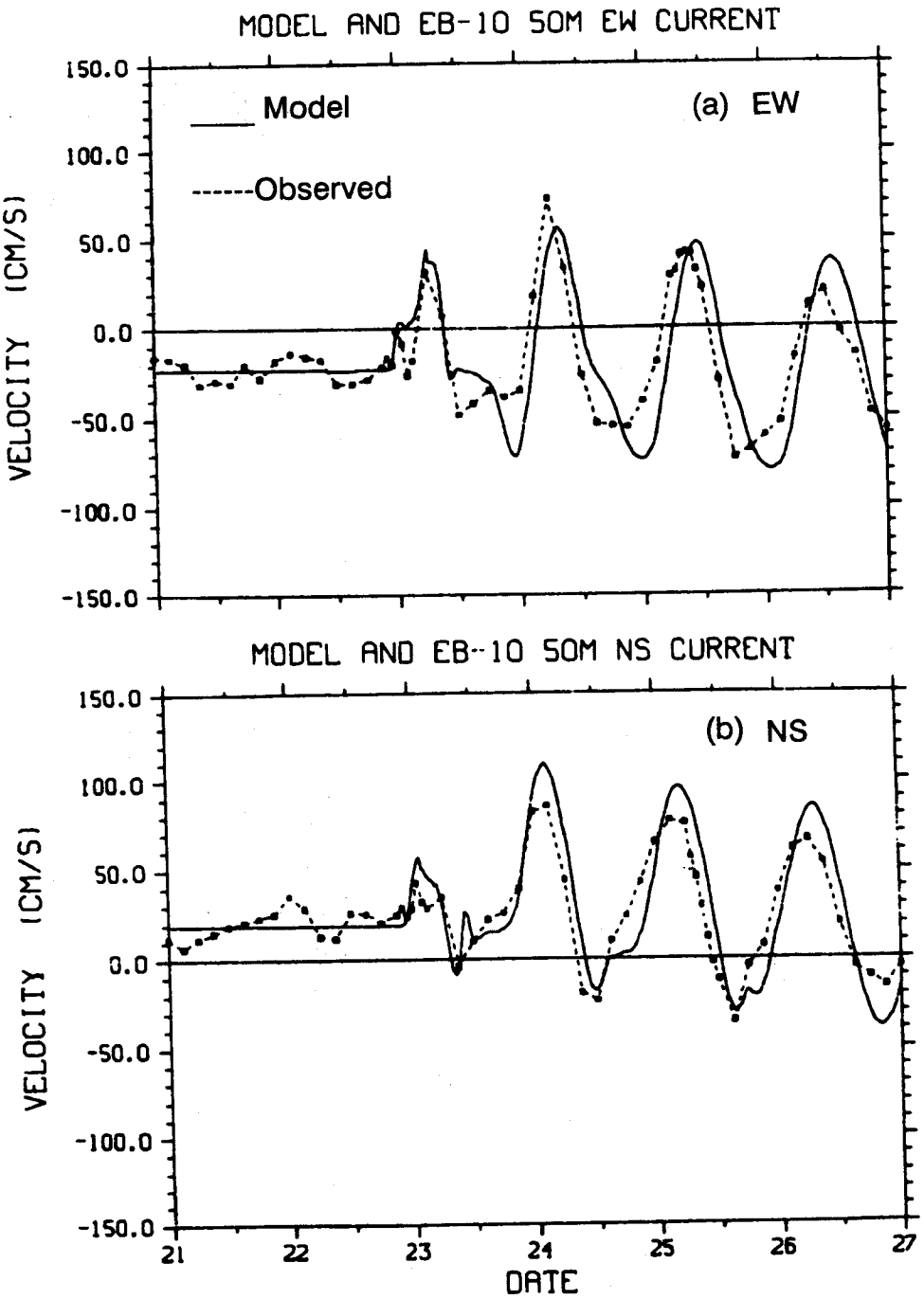

Figure 9. The mixed layer development under Hurricane Eloise (Martin, 1982).

The one that we are focusing on has the advantageous feature of being run operationally every day in conjunction with an objective analysis of all available data for the world's oceans. This system, called TOPS (thermodynamic ocean prediction system) (Clancy and Martin, 1981), encompasses a mixed layer model (formulated as a three-dimensional boundary layer model for the upper ocean), prognostic Ekman and inertial velocities (predicted by the mixed layer model), and a geostrophic velocity (provided by a diagnostic calculation or a prognostic forecast). The equations of this model (Warn-Varnas et al., 1984) take the form

$$\frac{\partial \overline{T}}{\partial t} = \frac{\partial}{\partial z}\left(\overline{-wT'} + \kappa \frac{\partial \overline{T}}{\partial z}\right) + \frac{1}{\rho w^c}\frac{\partial \overline{F}}{\partial z}$$
$$-\frac{\partial}{\partial x}(u_a\overline{T}) - \frac{\partial}{\partial y}(v_a\overline{T}) - \frac{\partial}{\partial z}(w_a\overline{T}) + A\left(\frac{\partial^2\overline{T}}{\partial x^2} + \frac{\partial^2\overline{T}}{\partial y^2}\right) \quad (1)$$

$$\frac{\partial \overline{S}}{\partial t} = \frac{\partial}{\partial z} m\left(\overline{-w'S'} + \kappa\frac{\partial \overline{S}}{\partial z}\right)$$
$$-\frac{\partial}{\partial x}(u_a\overline{S}) - \frac{\partial}{\partial y}(v_a\overline{S}) - \frac{\partial}{\partial z}(w_a\overline{S}) + A\left(\frac{\partial^2\overline{S}}{\partial x^2} + \frac{\partial^2\overline{S}}{\partial y^2}\right) \quad (2)$$

$$\frac{\partial \overline{u}}{\partial t} = f\overline{v} + \frac{\partial}{\partial z}\left(\overline{-w'u'} + \nu\frac{\partial \overline{u}}{\partial z}\right) - D\overline{u} \quad (3)$$

$$\frac{\partial \overline{v}}{\partial t} = -f\overline{u} + \frac{\partial}{\partial z}\left(\overline{-w'v'} + \nu\frac{\partial \overline{v}}{\partial z}\right) - D\overline{v} \quad (4)$$

where T is the temperature, S the salinity, u and v the x- and y-components of the current velocity (the x and y horizontal coordinates are defined relative to the grid), w the z-component of the current velocity, F the downward flux of solar radiation, r_w a reference density, c the specific heat of seawater, D a damping coefficient, ν a diffusion coefficient, f the Coriolis parameter, A the horizontal eddy diffusion coefficient, t the time, and z the vertical coordinate (positive upward from the level sea surface). Ensemble means are denoted by an overbar and primes indicate departure from these means. The quantities u_a, v_a are the x-, y-, and z- components of an advection current, which will be defined subsequently.

The advective terms are retained in the temperature and salinity equations and neglected in the momentum equations on the basis of scale analysis (Haney, 1974). Such an analysis shows that the advective terms in the thermal energy equations are of order unity, while the advective terms in the momentum equations are of the order of the Rossby number. Since the Rossby number is very small in most regions of the open ocean, the advective terms are dropped in the momentum equations.

Because there are no horizontal pressure gradient terms in Eqs. (3) and (4), u and v represent the wind-drift components of the current. Neglect of horizontal pressure gradients here is motivated by the fact that geostrophic currents generally do not play an important role inside the mixed-layer region which is the issue of most concern in this study.

The terms involving the damping coefficient D in Eqs. (3) and (4) represent the drag force caused by the radiation stress at the base of the mixed layer associated with the propagation of internal wave energy downward and away from the wind-forced region (Pollard and Millard, 1970; Niiler and Kraus, 1977)] The terms involving ν in Eqs. (1)-(4) account for very weak "background" eddy diffusion (due to intermittent breaking of internal waves, for example) that exists below the mixed layer. We take $D = 0.1$ day^{-1} and $\nu = 0.1$ cm^2 s^{-1} and note that these values are within the range of estimates for these quantities.

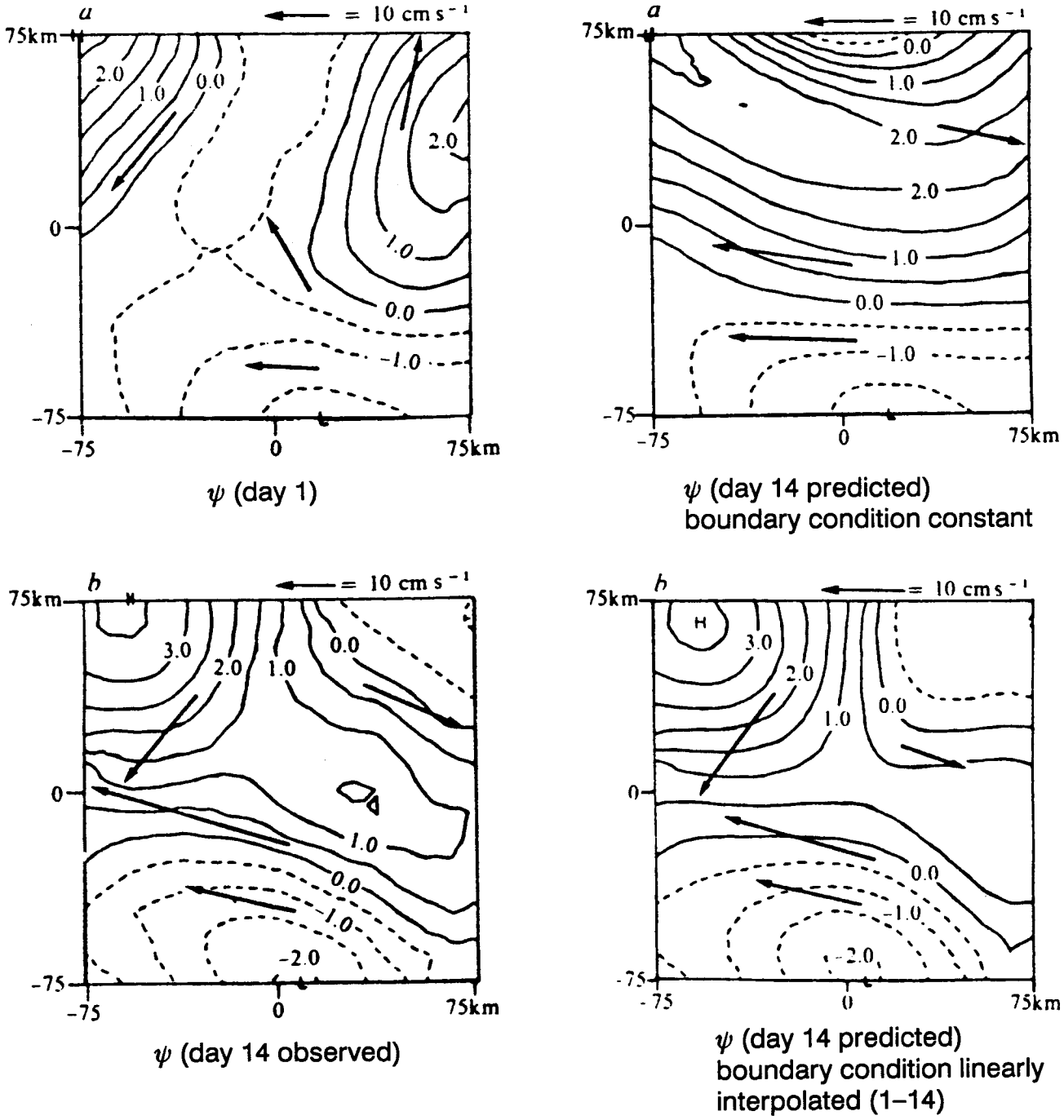

Figure 10. Example of a mesoscale ocean prediction experiment in the California Current (Robinson et al., 1986).

The Level-2 turbulence closure theory of Mellor and Yamada (1974) is used to parameterize the vertical eddy fluxes of temperature, salinity, and momentum. This turbulence model has been described in a number of papers (Mellor and Durbin, 1975; Clancy and Martin, 1981) and will not be presented here. Its energetics are essentially the same as those of Pollard et al. (1973) and Thompson (1976), with the increase in potential energy during mixed-layer deepening due to the buoyancy

flux at the layer base balanced locally by mean flow shear generation minus viscous dissipation of turbulent kinetic energy.

The horizontal eddy diffusion coefficient A is simply taken to be equal to a constant value of 10^7 cm^2 s^{-1}, and the divergence of the solar radiation flux is based on the data of Jerlov (1968) for seawater optical type 1A.

A vertically stretched grid of 17 points, extending from the level sea surface to 500 m depth, is used in the model. The horizontal grid, on which $\overline{T}$, $\overline{S}$, $\overline{u}$, $\overline{v}$, and w_a are defined, is a rectangular subset of the standard FNOC 63 x 63 Northern Hemisphere Polar Stereographic Grid.

The current used to advect the temperature and salinity is given by

$$ua = u_i + ug^*,\ va = v_i + vg^*,\ wa = w_i \qquad (5)$$

where u_i and v_i are the x- and y-components of the instantaneous wind-drift current, w_i is the vertical component of the current resulting from the divergence of u_i and v_i, and u_g^* are v_g^* are the components of a divergence-free geostrophic current.

The system TOPS provides information on the following environmental parameters: (a) Ekman and Inertial shears, (b) temperature and salinity profiles, (c) Brunt-Vaisala frequency, (d) Richardson number, (e) mixed layer depth, and (f) eddy coefficients

We have analyzed the archived forecasts of the TOPS prediction system for the year 1987. The analysis for environmental parameters was performed at eight former ocean station locations, Figure 11, with four locations each in the Pacific and the Atlantic, respectively. Figure 12 shows the monthly averaged mixed layer depth at the eight stations. Observe the almost simultaneous spring shallowing around the May-June period, and the more diverse fall deepening. Another striking feature of these results is the much deeper winter values of the MLD (mixed layer depth) in the Atlantic than in the Pacific, due to the presence of a halocline in the latter than tends to inhibit deep mixing in the winter. Figure 13 exhibits the simulated seasonal shear at ocean station Papa in the Atlantic. Note that the maximum shear occurs in the summer. This happens because during the summer the mixed layer is shallow and contains the momentum generated by the atmospheric forcing at the surface (in the winter the momentum is contained in a deeper mixed layer).

CONCLUSION

We advocate the use of upper ocean and mesoscale models to provide the deterministic part of the forecast of the environmental parameters. There are aspects of internal wave statistics and their non-stationarity which can be predicted by thermodynamic and hydrodynamic models of ocean circulation. Figure 14 elucidates the proposed approach. Internal wave activity depends on Brunt-

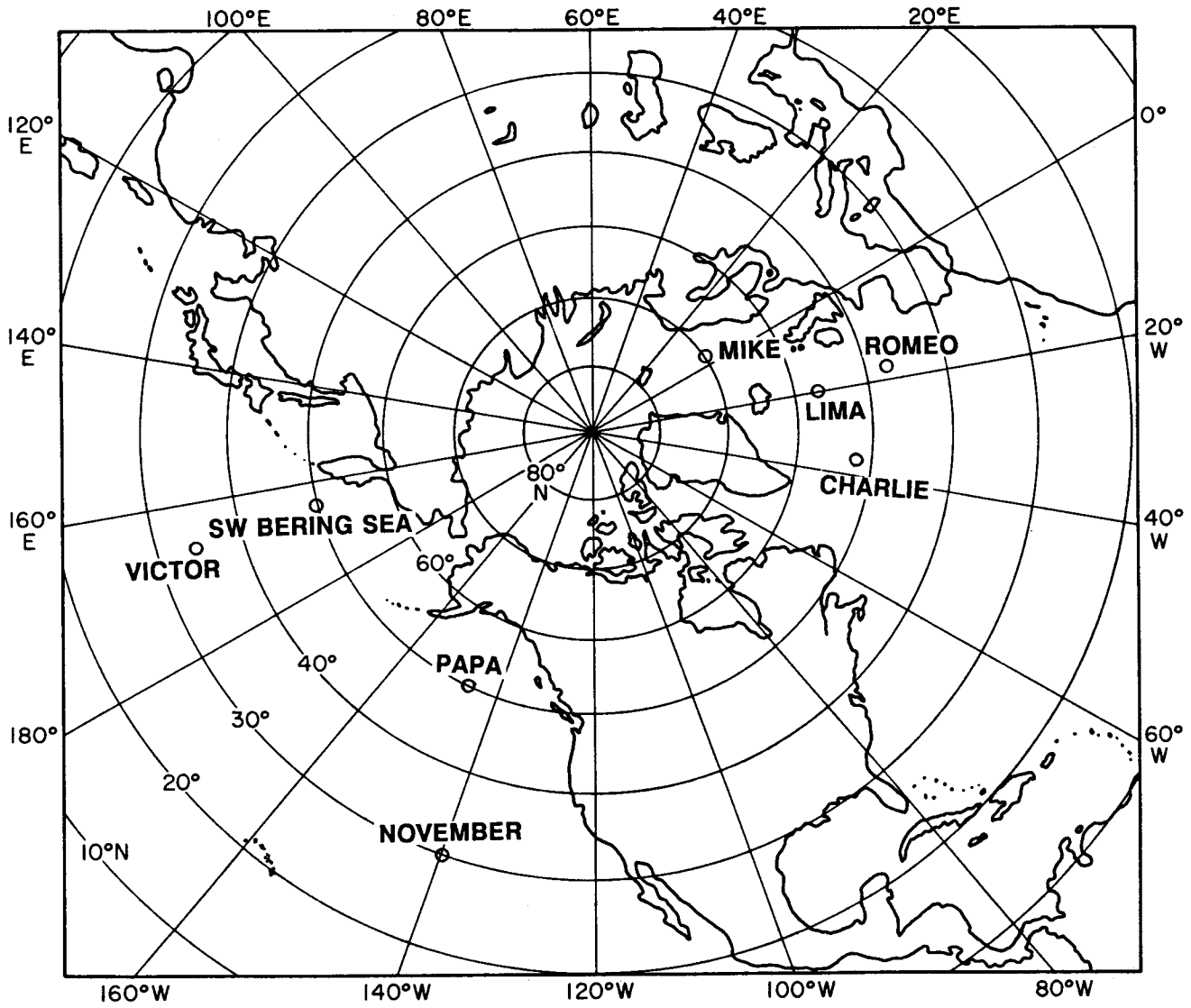

Figure 11. Locations of the three weather ships and one TOPS model grid in the North Pacific, and of the 4 weather ships in the North Atlantic, where XBT observations and routine model predictions have been carried out with the TOPS operational 3-D mixed layer model.

Vaisala frequency times a non-dimensional parameter (Briscoe and Weller, 1984; Rubenstein, 1984). Thus the model -forecasted Brunt-Vaisala frequency will enable us to calculate the internal wave activity.

Furthermore, we propose to: (a) collect statistics on internal wave and fine structure, (b) determine the critical environmental parameters on which the statistics depend, and (c) use the statistical empirical relations together with the model forecast to determine the environmental parameters of interest in terms of the mean and the deviations.

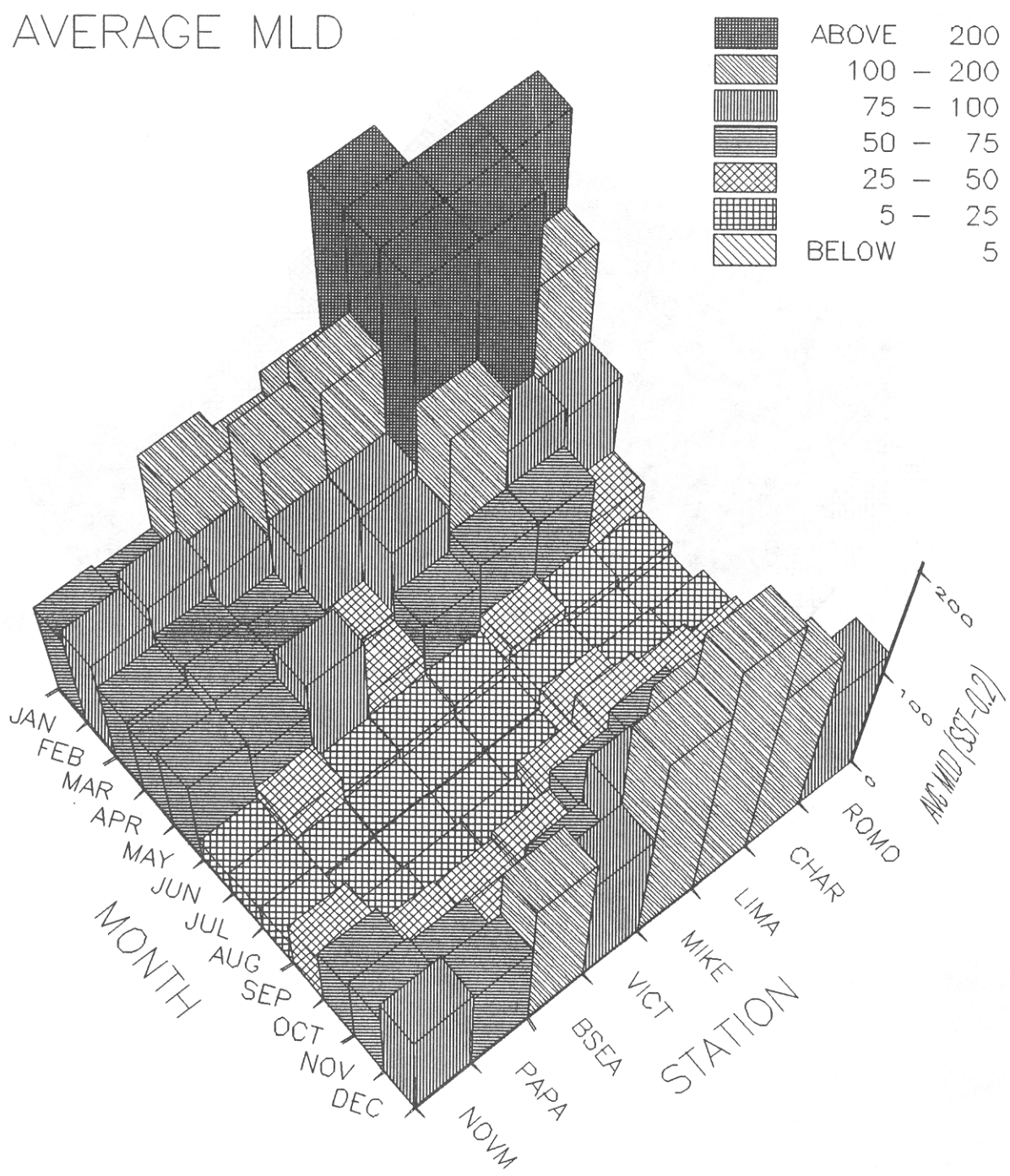

Figure 12. The average mixed layer depth (MLD) at the 8 locations illustrated in Figure 11 for the year 1985, as obtained by the operational model TOPS forced by GCM fluxes and updated by analyzed temperature fields using all available XBT's (Piacsek et al., 1988).

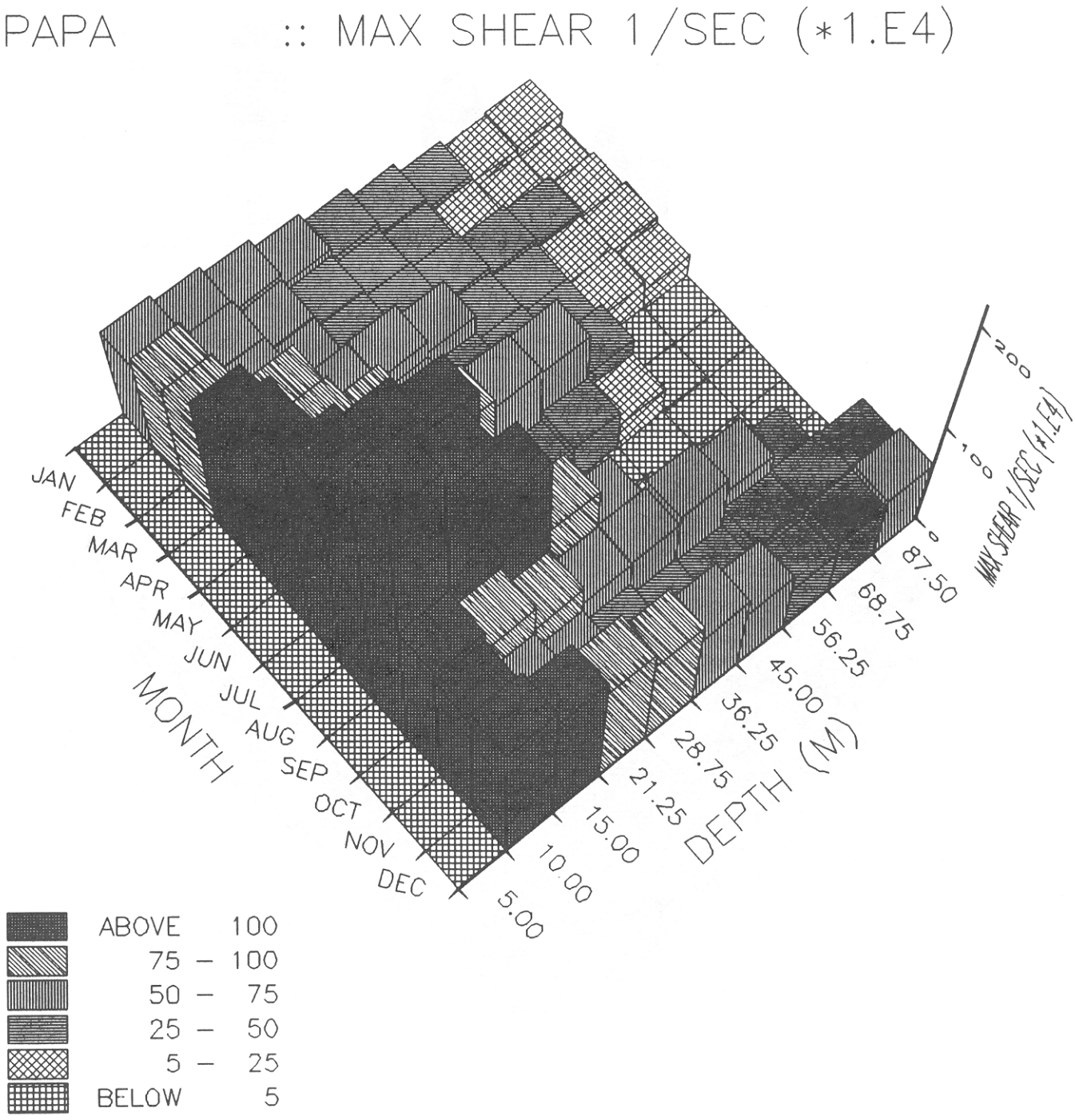

Figure 13. The maximum vertical shear at the eight locations illustrated in Figure 11 for the year 1985, as obtained by the operational model TOPS forced by GCM fluxes and updated by analyzed temperature fields using all available XBT's (Piacsek, 1988).

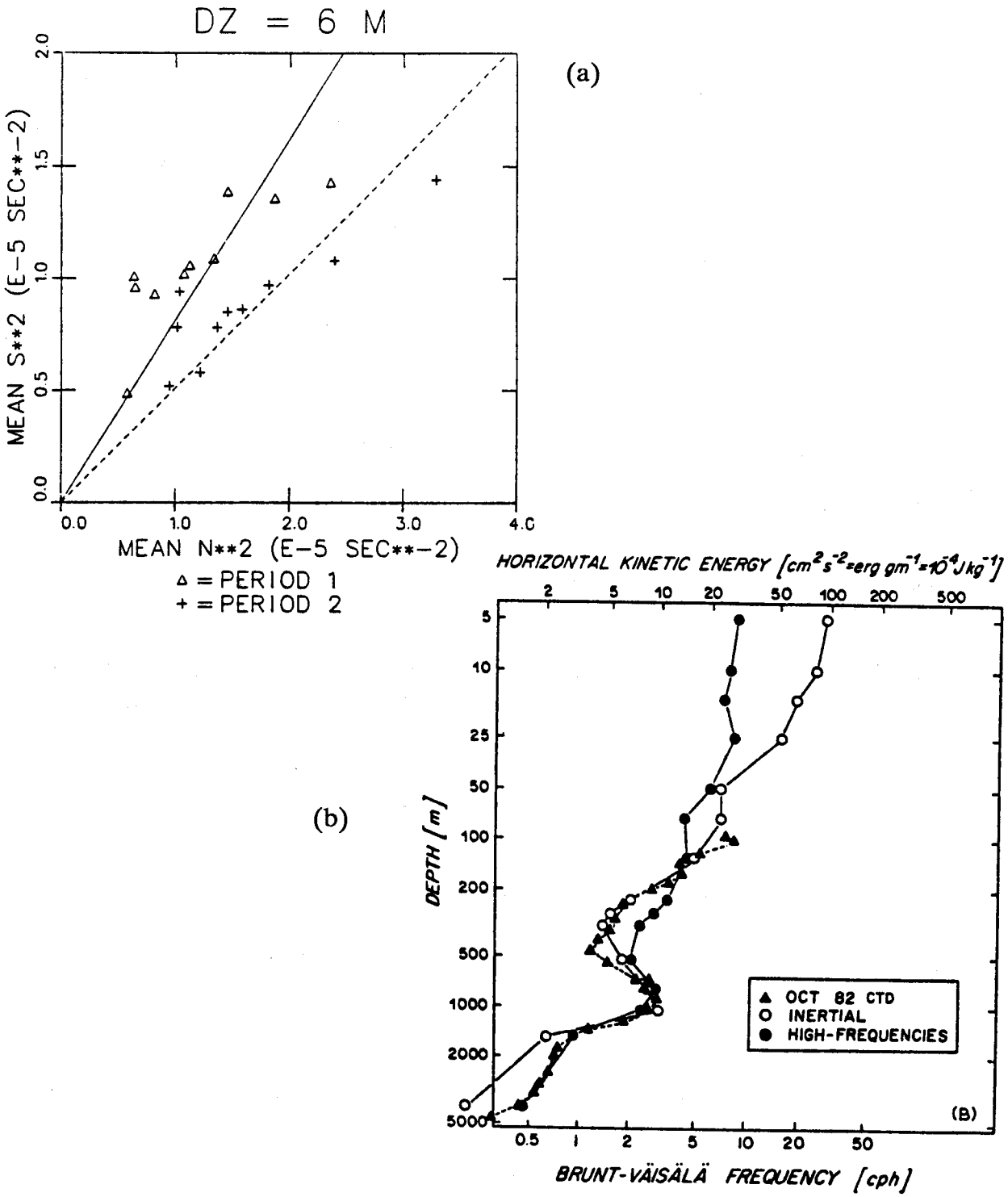

Figure 14. (a) The mean-square shear across 6m intervals vs. BV frequency during period 1 (31 July to 9 August 1978) and period 2 (23 Aug to 6 Sept 1978) (Rubinstein, 1984).
(b) Profiles of inertial and high-frequency internal wave energy together with the BV profile for October 1982 in the Hatteras abyssal plain, showing the WKB scaling of energy (Briscoe and Weller, 1984).

REFERENCES

Boyd, J.D. and H. Perkins, 1987: Characteristics of thermohaline steps off the northwest coast of South America. *Deep-Sea Res.* 337-364.

Brown, E.D. and W.B. Owens, 1981: Observations of the Horizontal Interactions between the Internal Wave Field and the Mesoscale Flow, *J. Phys. Oceanogr.* 11:1474-1480.

Briscoe, M., 1983: Observations on the energy balance of internal waves during JASIN, *Phil. Trans. Royal Soc. London*, Ser A: 308, p. 427-444.

Briscoe, M.G. and R.A. Weller, 1984: Preliminary Results from the long-term upper ocean study (LOTUS), *Dynamics of Atmospheres and Oceans* 8:243-265.

Clancy, R.M. and K.D. Pollak, 1983: A Real-Time Synoptic Ocean Thermal Analysis/Forecast System, *Prog. Oceanogr.* 12:383.

Clancy, R.M., 1987: Real-Time Applied Oceanography at the Navy's Global Center, *Mar. Tech. Soc. Journal* 21:33.

Clancy, R.M. and P.J. Martin, 1981: Synoptic Forecasting of the Oceanic Mixed Layer Using the Navy's Operational Environmental Data Base: Present Capabilities and Future Applications, Bull. AMS 62, p. 770.

Garrett, C. and W. Munk, 1975: Space-Time Scales of Internal Waves: a Progress Report, *J. Phys. Oceanogr.* 80:291-297.

Garwood, R.W., 1977: An oceanic mixed-layer model capable of simulating cyclic states, *J. Phys. Oceanogr.* 7:455-468.

Haney, R.L., 1974: A numerical study of the response of an idealized ocean to large-scale fluxes of heat and momentum flux, *J. Phys. Oceanogr.* 4:145-167.

Hopkins, T.S., P. Povero and S. Piacsek, 1989: Upper layer environmental parameters from CTD data -GIN '86 Cruise, SACLANT Research Center memorandum SM-225, December 1989.

Jerlov, N.G., 1968: *Optical Oceanography*, Elsevier Press, New York, 352 pp.

Martin, P.J., 1982: Mixed-Layer Simulation of Buoy Observations Taken During Hurricane Eloise, *J. Geophys. Res.* 87:409-427.

Martin, P.J., 1985: Simulation of the Mixed Layer at OWS November and Papa with Several Models, *J. Geophys. Res.* 90:903-916.

Mellor, G.L. and T. Yamada,, 1974: A hierarchy of turbulence closure models for planetary boundary layers, *J. Atmos. Sci.* 31:1791-1806.

Mellor, G.L. and Durbin, P.A., 1975: The structure and dynamics of the ocean mixed layer, *J. Phys. Oceanogr.* 5:718-728.

Niiler, P.P., 1975: Deepening of the wind-mixed layer, *J. Mar. Res.* 33:405-422

Niiler, P.P. and E.B. Kraus, 1977: One-dimensional models of the upper ocean. In: *Modeling and prediction of the upper layers of the ocean.* E.B. Kraus, ed., Pergamon Press, Oxford, p. 143.

Piacsek, S.A. and G.O. Roberts, 1975: Numerical Experiments on Collapsing Wakes in a Stratified Fluid, NRL Tech. Mem. #3178, 67 pp.

Piacsek, S.A., L. Henderson, P. VanMeurs, A. Warn-Varnas, and J. French, 1988: *Operational Prediction of Upper Ocean Environmental Parameters*, NORDA Tech. Note 379, April 1988, 102 pp.

Pollard, R.T. and R.C. Millard, 1970: Comparison between observed and simulated wind-generated inertial oscillations. *Deep-Sea Res.* 17:813-821.

Pollard, T.R., P.B. Rhines, and R.O.R.Y. Thompson, 1973: The deepening of the wind driven mixed layer, *Geophys. Fluid Dyn.* 3:381-404.

Price, J.F., 1981: Upper Ocean Response to a Hurricane, *J. Phys. Oceanogr.* 11:153-175

Price, J.F., R.A. Weller and R. Pinkel, 1986: Diurnal Cycling: Observations and Models of the Upper Ocean Response to Diurnal Heating, Cooling and Wind Mixing. *J. Geophys. Res.* 91:8411-8425.

Robinson, A.R., J.A. Carton, N. Pinardi, and C.N.K. Mooers, 1986: Dynamical Forecasting and Dynamical Interpolation: An Experiment in the California Current, *J. Phys. Oceanogr.* 16:1561-1579.

Ruddick, B.R. and T.M. Joyce, 1979: Observations of Interaction between the Internal Wavefield and Low-Frequency flows in the North Atlantic, *J. Phys. Oceanogr.* 9:498-517.

Rubenstein, D.M., 1984: Upper Ocean Shear During JSAIN: A Deterministic and Statistical Analysis, Science Applications, Inc. Tech. Rep. SAI-84/1027, Feb. 1984.

Sellschopp, J., 1987: Towed Thermistor Chain Data collected during the cruise "NORDMEER 87", FWG Report 1987-4, Forschungsanstalt der Bundeswehr fur Wasserschall-und Geophysik, Kiel, Germany.

Thompson, R.O.R.Y., 1976: Climatological numerical models of the surface layers of the ocean. *J. Phys. Oceanogr.* 6:496-503.

Warn-Varnas, A., G.M. Dawson, and P.J. Martin, 1981: Forecast and Studies of the Oceanic Mixed Layer During the MILE Experiment, *Geophys. Astrophys. Fluid Dyn.* 17:63-85.

Warn-Varnas, A., R.M. Clancy, M.L. Morris, P.J. Martin, and S. Horton, 1984: Studies of Large-scale Thermal Variability with Synoptic Mixed-Layer Model, in *Predictability of Fluid Motions*, G. Holloway, ed., American Institute of Physics, Conf. Proc. #106, p. 515-535.